Journal of Electronic Materials (2022) 51:4388–4406
https://doi.org/10.1007/s11664-022-09668-7

ORIGINAL RESEARCH ARTICLE

# Time to Failure Prediction on a Printed Circuit Board Surface Under Humidity Using Probabilistic Analysis

**Sajjad Bahrebar**[1] · **Rajan Ambat**[1]

Received: 8 December 2021 / Accepted: 20 April 2022 / Published online: 18 May 2022


## Abstract

This paper presents the probabilistic study of time to failure (TTF), which is caused by combinations of various important controllable factors on a printed circuit board (PCB) surface under humidity. The study investigated the impact of four changeable factors including pitch distance, temperature, contamination, and voltage, each at three levels upon the surface insulation resistance test boards. Constant 98% relative humidity with adipic acid as contamination related to flux residue was used for a 20-h parametric experiment. Two main states were considered on the whole output current measurements: the stable part before the short transition phase and the unstable part after due to electrochemical migration (ECM) on the PCB surface. Leakage current (LC) in the first state and TTF at the beginning of the second stage was measured with five replications for each condition as the predictive indicator in all models. The trend of LC and TTF was also investigated on three levels of each factor. In addition, probabilistic distribution analysis using fitted Weibull distribution, multivariate regression analysis, and the classification and regression tree (CART) analysis were used to predict the probability of TTF and failure risk prediction on the PCB surface. All the prediction models had an acceptable prediction of TTF at diverse accuracy levels, according to changing factors/levels. Nevertheless, the multivariate regression analysis had the best prediction, highest $R^2$, and lowest error compared to the other models.

**Keywords** Probabilistic analysis · prediction model · probability of failure · PCB surface · time to failure

## Introduction

Development in electronics usage had caused an increase in the user demand for robust performance in various environments, while miniaturization is occurring at the system, printed circuit board assembly (PCBA), and component level.[1] The use of a smaller component size is growing due to PCBA miniaturization, which causes a higher electric field compared to a larger size when exposed to humid conditions resulting in water film formation.[2] The increase in component density and their influence on each other under space reduction on the PCBAs is a challenging issue today especially for use under harsh conditions.[3] Many of the small-sized electric components consequently have smaller pitch distances that play an important role in their failure mechanisms.[4,5] Hence, pitch distance (P) is considered a critical factor with a direct effect on increasing or decreasing the time to failure (TTF) on PCBAs when exposed to various climatic conditions. It refers to the spacing between two oppositely charged conduction lines or between electrodes of a component on PCBAs.

The soldering process, especially wave soldering, introduces contamination during manufacturing, which together with other factors influences the humidity-related corrosion failure on the PCB surface.[6,7] Moreover, the hygroscopic nature of the flux residue changes the humidity boundary for water film formation when exposed to a climatic profile during operation.[8] Adipic acid is an active component in flux residue that could have different deliquescence relative humidity (DRH) and efflorescence relative humidity (ERH) levels depending on the chemistry.[9] Hence, contamination (C) is another critical factor for failure creation on the PCB surface under exposure to humidity. Generally, contamination on a PCB surface originates from three cases, namely, (i) manufacturing processes such as flux residue as described

✉ Sajjad Bahrebar
sajbahr@mek.dtu.dk

[1] Department of Mechanical Engineering, Center for Electronic Corrosion, Section of Materials and Surface Engineering, Technical University of Denmark, 2800 Lyngby, Denmark

before; (ii) service-related contamination, for example, atmospheric particles settling on the PCB surface; and (iii) handling of a PCB that may leave finger prints resulting from handling without gloves.[10] Among these, the manufacturing process is the most important contamination source as the other two sources are mostly removed by careful handling and proper packaging. Manufacturing processes related contamination could again be divided into that originating from base PCB manufacturing and PCB assembly. The PCB assembly process is the last process, and the no-clean flux results in a dominating factor for contamination.

The climatic conditions have a fundamental role in the initial failure process on the PCB surface. Climatic conditions refers to level of humidity, temperature, and their variations. These two factors can determine the water vapor range that starts to condense on the PCB surface. Additionally, this water condensation is also dependent on the hygroscopic nature of ionic residues from soldering under transient conditions of varying humidity and temperature.[11] Therefore, the temperature (T) is another important factor on the PCB surface. Furthermore, temperature plays a crucial role in accelerating the corrosion of metallic materials on the PCB surface.[12] It should be noted that in this study only the temperature is considered in different levels, while keeping the humidity above the deliquescent humidity level proportional to the adipic acid as the only contamination type.[13]

The water layer formation due to pitch distance, ionic contamination remaining from the soldering process, change in climatic conditions, and surface material properties lead to surface insulation resistance (SIR) reduction on the PCB surface if closely spaced biased points are connected. The thin water layer formation easily acts as a conductor by making electrochemical cells for corrosion failure mechanisms.[14] By applying a voltage, an electric field is made through the thin water layer, subsequently leading to corrosion failure in the form of dendrite formation due to ECM on the PCB surface. This event will cause a sudden increase in the leakage current (LC), resulting in the operational capacity of the PCBs. Thus, voltage (V) is considered another critical factor that creates a distinct potential bias between the anode and cathode and makes the migration of anodic metal ions in the conductive water layer and subsequent deposition at the cathode.[15]

In this study, the pitch distance levels of 300 µm, 600 µm, and 1000 µm as P1, P2, and P3 are considered proportional to actual surface mount device (SMD) components. As an important weak organic acid (WOA), adipic acid is studied for all experiments in three contamination levels of 50 µg/cm$^2$, 75 µg/cm$^2$, and 100 µg/cm$^2$ as C1, C2, and C3 matching with typical levels of flux residues usually seen after the wave soldering process.[16] The temperature is varied at three levels, 40°C, 45°C, 50°C, while keeping the humidity level above the deliquescent relative humidity level (98%) for the adipic acid. In addition, three levels of voltage have been considered for this study, namely, 5 V, 7.5 V, and 10 V matching with input voltage range of low-power components and devices.[17] Figure 1 presents the overview of short circuit failure mechanisms between biased points on the PCB surface and critical factors of its failure causes.

Different studies have focused on the effect of climate conditions at various potential biases,[18,19] as well as the effect of PCB surface failure and contamination types.[20,21] Nonetheless, only a limited body of research has experimentally investigated failure prediction on PCBs[22,23] while there is no discussion about all of the critical factor effects and TTF prediction using probabilistic approaches at critical conditions, along with combination factors. While the probabilistic approach provides the required methods and tools for reliability and risk assessment,[24] it works well in lifetime prediction and the estimation of the probability of failure of electronic components as well.[25] For the humidity robustness of electronic devices, it is also important to predict and determine TTFs. Usually, the probabilistic approaches are applied for the reliability assessment of electronics devices,

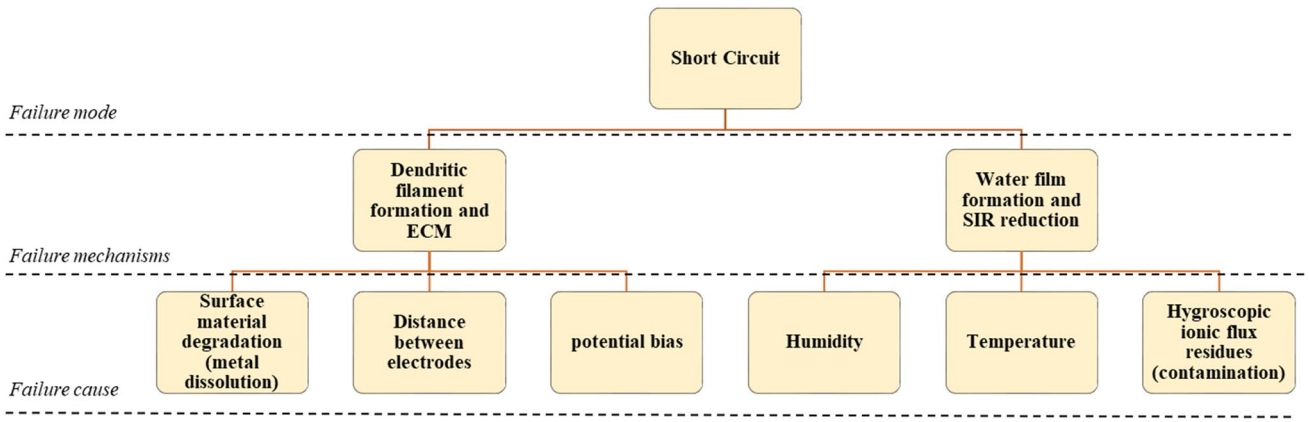


**Fig. 1** Failure mechanisms and failure causes of short circuit as the main failure mode on the PCB surface.

predicting TTFs and quantifying the probability of failures at various conditions.

Accordingly, this study addresses the probabilistic approach of various controllable factors influencing the TTF due to ECM on PCB surface, as well as the resulting probability of failure (PoF) and risk prediction at various conditions. The outcomes are monitored as an evaluation criterion for four appraised and changeable factors of pitch distance, contamination, temperature, and voltage, each at low, medium, and high levels. Additionally, 98% (RH) and one kind of important contamination (adipic acid) for a 20-h experimental period as constant factors are considered on the SIR test boards. The effects of factors/levels with five replications in each condition on TTFs and LCs and their relationship are statistically studied in the primary step. Focusing more on pitch distance and temperature as the two most significant factors, the best understanding of these two factor effects has been obtained on the PCB surface failure. In the next step, using probabilistic distribution analysis, the appropriate probability distribution for each condition according to three approaches, based on the nature of data, probability plotting, and analytical techniques have been investigated. Using goodness-of-fit tests (i.e., Chi-square, Anderson-Darling, and Kolmogorov-Smirnov tests) and maximum likelihood methods, the Weibull distributions as the main distribution for life prediction on the accelerated tests compared to other distributions (e.g., exponential and lognormal distributions) have been selected on all TTFs. Furthermore, four periods of time, namely, highly fast (under 1 h), fast (between 1 and 4 h), medium (between 4 h and 7 h), and slow (over 7 h) to reach the TTF are considered for estimating the PoF for each condition. Next, the classification and regression tree (CART) analysis, a supervised machine learning method, is used to classify and predict TTF data based on changeable factors. In addition, a multivariate regression analysis is applied to identify a formula that can explain how factors influence TTF with deterministic and probabilistic data of every 21 different experimental conditions. Finally, a combination of statistical, probabilistic distribution, multivariate regression, and CART analyses have provided a complete understanding of critical factors, levels, and conditions for having the best TTF probability prediction knowledge on PCB surfaces.

## Material and Methods

### Method and Experiment Design

The one-factor-at-a-time (OFAT) method is a traditional design in which all factors are considered constant variables, and only the effect of one factor is measured on the response.[26] Hence, the conclusion of OFAT experimental results represents the one-factor behavior effect without any interaction effect.[27] Table I presents the three different levels of each important and changeable factor (pitch distance, contamination, temperature, and voltage) with their units and symbols. The constant level of each factor in every vertical column (P2, C3, T2, V3) is shown in red. Furthermore, the horizontal rows display the low, medium, and high levels of each factor, and the horizontal column shows three new conditions at each level. If there are four factors, each at three levels, then the number of experiments in the OFAT method will be equal to nine different experimental conditions.[28] In other words, 45 experiments in vertical conditions (nine different conditions), and 15 different experiments in horizontal conditions (three different conditions), in addition to 10 more experiments for two specific conditions on pitch distance and temperature factors due to the existing high effect on responses, are specified (14 different experimental conditions) in this study. Six out of these 14 experimental conditions (P1a100c45v10, P1a100c50v10, P2a100c45v5, P2a100c45v10, P2a100c50v10, and P2a50c45v10) are partly retrieved in this study from our previous work.[29] For example, P1a100c50v10 represented the low level of pitch distance and the high level of other factors (P1, small pitch distance; a100, high level adipic acid as contamination; c50, high level temperature; v10, high level voltage). In two specific experiments only for pitch distance and temperature as the two most significant factors (instead of the constant condition C3, T2, V3), another experimental condition with a different level of temperature (C3, T3, V3) is investigated for the pitch distance column. Similarly, in addition to the

**Table I** Three levels of four critical factors for performing the OFAT experiments

| Level | Pitch Distance | Contamination | Temperature | Voltage | *Horizontal Condition* |
|---|---|---|---|---|---|
| **Low** | P1 (300 µm) | C1 (50 µg/cm²) | T1 (40 °C) | V1 (5 V) | *P1, C1, T1, V1* |
| **Medium** | P2 (600 µm) | C2 (75 µg/cm²) | T2 (45 °C) | V2 (7.5 V) | *P2, C2, T2, V2* |
| **High** | P3 (1000 µm) | C3 (100 µg/cm²) | T3 (50 °C) | V3 (10 V) | *P3, C3, T3, V3* |
| *Vertical conditions* | *C3, T2, V3*<br>*C3, T3, V3* | *P2, T2, V3* | *P2, C3, V3*<br>*P1, C3, V3* | *P2, C3, T2* | |

constant condition (P2, C3, V3), another condition with P1 (P1, C3, V3) is measured for the temperature column.

The current behavior as an important indicator is measured to define LC and TTF on the PCB surface. Figure 2 depicts the general current behavior of the entire experimental results, assuming two main parts and specifying two responses. First, there are LCs in the SIR reduction part, and second, TTF points in the initial failure part. The SIR reduction part (the stable part) is assigned to LC, and the failure part (the unstable region), is referred to start the failure process on PCB surfaces with a large jump in LC. The effects of factors/levels on TTFs and LCs and their relationship are statistically evaluated in the initial part of the paper, while the modeling part focused only on TTFs predictions.

## Specimens, Preparations, and Test Equipment

SIR comb patterns are commonly used and their measurements are the usual test methods for the process of reliability and quality control.[30,31] Figure 3 displays the individual SIR patterns that included three different surface areas and three pitch distances made on FR-4 laminate with a thickness of 1.6 mm complying with the IPC-4101/21 standard. The SIR patterns have three pitch distances, namely, 0.3 mm, 0.6 mm, and 1 mm. They are proportional to actual distances on a typical PCBA. The dimensions, areas, and pitch distances of each SIR pattern are displayed in Fig. 3.

In preparation before starting the test, the PCBs are cleaned and then dried by an air compressor using a combination of deionized water and isopropanol. Then, each SIR pattern is contaminated with a solution of 2.5 g adipic acid dissolved in 100 mL isopropanol at a concentration of 25 g/L. An appropriate amount of this solution was dispensed on the surface of SIR patterns using a micropipette and dried in order to obtain contamination levels 50 µg/cm$^2$, 75 µg/cm$^2$, and 100 µg/cm$^2$ matching with typical levels of flux residues usually seen after the wave soldering process.

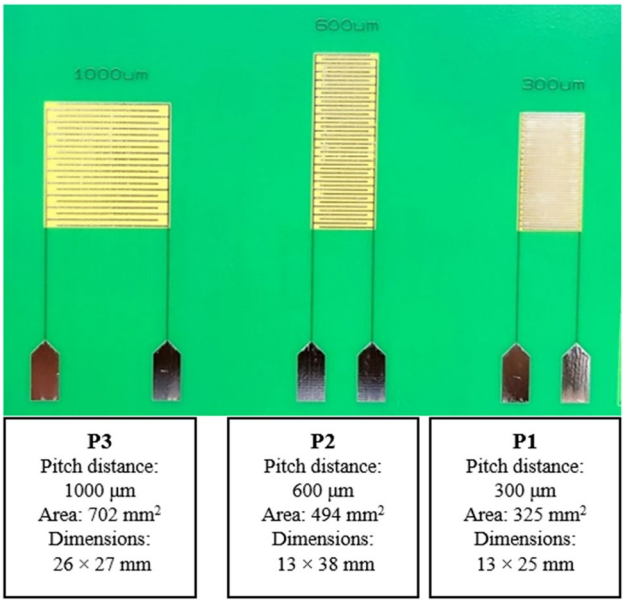


**Fig. 3** The overall view of SIR pattern PCB test boards with three different pitch distances.

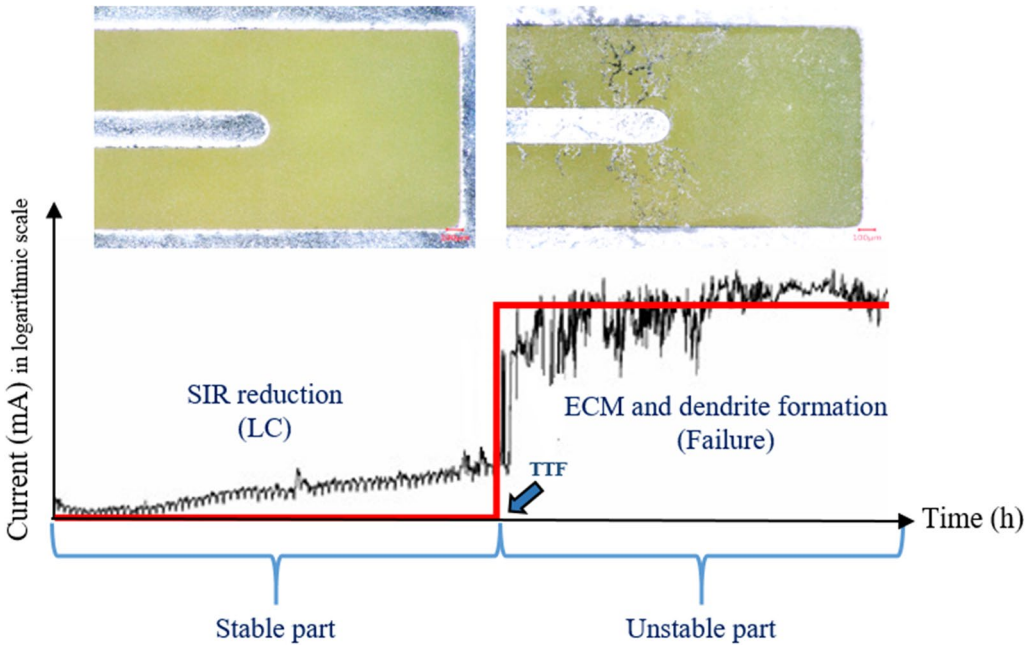


**Fig. 2** The overall current behavior on exposure to various conditions with the actual pictures of the PCB electrodes of two main regions.

Electrical connection to the PCB board is made by hand soldering of wires to the electrical contacts on the board.

All experiments are performed inside an Espec climatic chamber with the tolerances of ±0.3°C and ±2.5% RH. In accordance with the adipic acid as contamination during the tests, the RH (proportional to the deliquescence data) was kept constant at 98% for the experiments. For each experiment, a 1.5-h period is used in the climatic chamber before each test as the stabilization period. A multichannel Bio-Logic VSP system is used for the application of potential (5 V, 7.5 V, and 10 V) and accurate measurement of leakage current.

## Multivariate Regression Model

The multivariate regression model is a mathematical function which pursues a logical relationship between different significant variables by statistical estimation and analysis of variance (ANOVA).[32,33] The multivariate regression model has been used for analyzing the statistical significance of four critical factor effects and for determining a significant correlation in terms of multiple factors.[34] The backward elimination stepwise investigation has been performed through multivariate regression analysis for making a reduced model on TTFs based on significant factors.[35]

## Probabilistic Distribution Analysis

The probability concept constructs the core of risk and reliability engineering, and the probabilistic approach is the key to assessing risk and reliability by providing the needed techniques and methods.[32] The probabilistic distribution analysis has been used to achieve a mathematical function that gives the probabilities of TTFs and estimates the risk presented by the various conditions. It starts with assumptions about selecting an appropriate distribution. Usually, three approaches are used to select an appropriate and applicable probabilistic distribution. The initial action for selecting the distribution relies on the nature of the data. For example, Weibull distribution is generally used to predict lifetime at accelerated tests.[33] The second approach is probability plotting as an approximate method to provide sensible rationales for choosing the proper distribution. The third approach is analytical procedures to determine how appropriate the selected probability distribution signifies the data set.[36] Generally, finding a specific distribution for various experimental conditions on diverse TTFs is impossible. However, Weibull distribution, compared with other distributions (e.g., exponential distribution), is selected for TTF data sets at each condition separately. It implies that the exponential distribution that is a useful distribution for life prediction in accelerated tests with a single parameter (failure rate λ) is unsuitable for these TTF data sets. Moreover, maximum likelihood methods and goodness-of-fit tests comprising Chi-square, Kolmogorov-Smirnov, and Anderson-Darling tests as analytical techniques have determined the properly fitted Weibull distribution on TTF data.[36,37]

Weibull distribution is one of the most desirable distributions for a continuous event due to its flexibility and adaptability for modeling data with a negligible amount of failures. It is specifically used for failure prediction in the accelerated life tests.[38,39] The Weibull distribution can provide accurate failure analysis and risk calculations with a few samples without taking too much data.[40] The probability density function (PDF) of the three-parameter (3P) Weibull distribution is presented as follows[40]:

$$f(t) = \frac{\beta}{\alpha - \theta}\left(\frac{t-\theta}{\alpha-\theta}\right)^{\beta-1} \cdot \mathrm{Exp}\left[-\left(\frac{t-\theta}{\alpha-\theta}\right)^{\beta}\right]$$

where $\theta$ (theta) is the location parameter, $\alpha$ (alfa) is a measure of the range and the characteristic value. $\beta$ (beta) is the slope or shape parameter, which designates whether the failure rate is increasing, constant, or decreasing and follows the following rules[41,42]:

$\beta < 1 \Rightarrow$ Determines that the product has a decreasing failure rate.

$\beta = 1 \Rightarrow$ Determines a constant failure rate (exponential distribution).

$\beta > 1 \Rightarrow$ Determines an increasing failure rate. (This is typical of products that are wearing out, and the property of normal distribution is exhibited when $\beta \sim 3.5$.)

## CART Analysis

CART analysis is a supervised machine learning algorithms that provides insight into a wide range of applications such as manufacturing quality control, and the result is applied to identify important variables and predict response values.[43,44] This method as a decision tree illustrates important relationships between a response and important predictors, in which each branch is split among a predictor, and each end node contains a prediction for the response.[45] CARTanalysis has been used for creating a predictive model of the dependent variable (TTF) based on the independent variables (P,C,T,V). In addition, it has been performed through classification as a qualitative prediction at four hypothetical periods of time, followed by discussing the regression tree for TTF responses as a quantitative prediction in terms of changeable factors in this study.

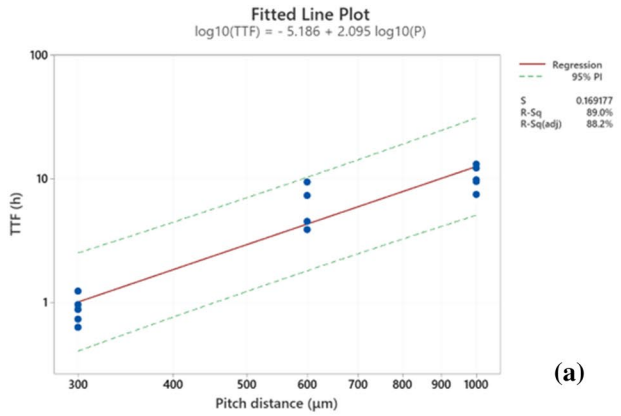
Fitted Line Plot
log10(TTF) = - 5.186 + 2.095 log10(P)
Regression
95% PI
S 0.169177
R-Sq 89.0%
R-Sq(adj) 88.2%
TTF (h)
Pitch distance (µm)

(a)

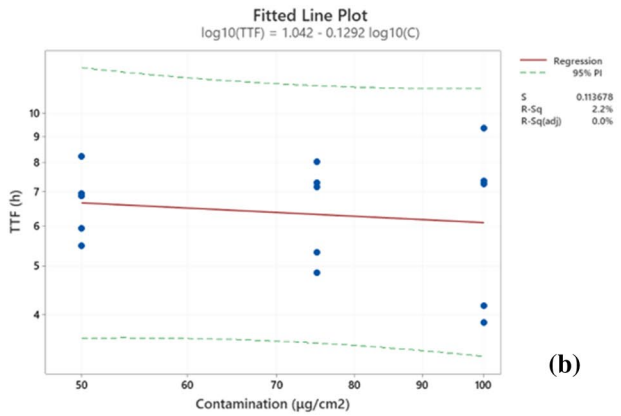
Fitted Line Plot
log10(TTF) = 1.042 - 0.1292 log10(C)
Regression
95% PI
S 0.113678
R-Sq 2.2%
R-Sq(adj) 0.0%
TTF (h)
Contamination (µg/cm2)

(b)

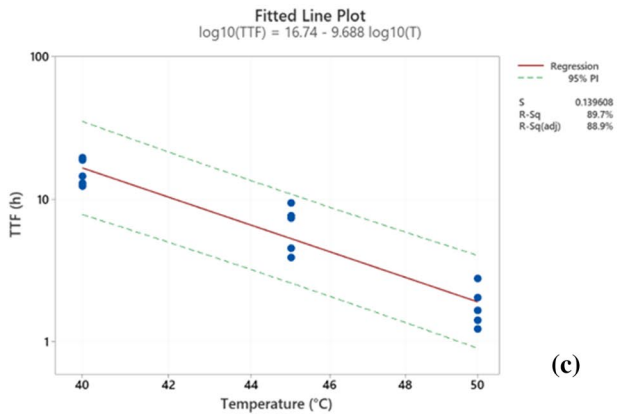
Fitted Line Plot
log10(TTF) = 16.74 - 9.688 log10(T)
Regression
95% PI
S 0.139608
R-Sq 89.7%
R-Sq(adj) 88.9%
TTF (h)
Temperature (°C)

(c)

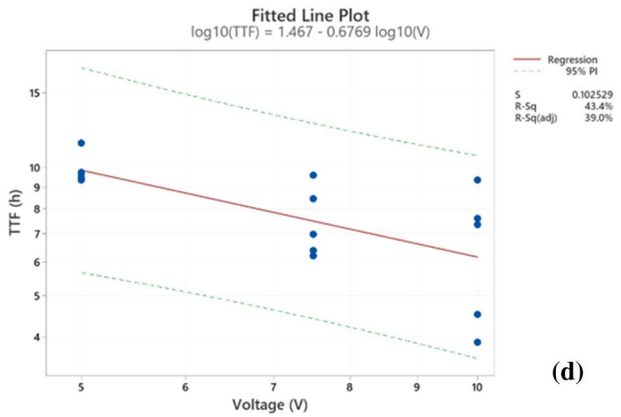
Fitted Line Plot
log10(TTF) = 1.467 - 0.6769 log10(V)
Regression
95% PI
S 0.102529
R-Sq 43.4%
R-Sq(adj) 39.0%
TTF (h)
Voltage (V)

(d)

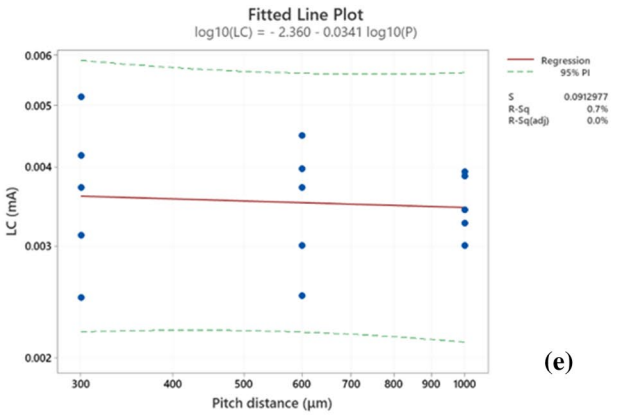
Fitted Line Plot
log10(LC) = - 2.360 - 0.0341 log10(P)
Regression
95% PI
S 0.0912977
R-Sq 0.7%
R-Sq(adj) 0.0%
LC (mA)
Pitch distance (µm)

(e)

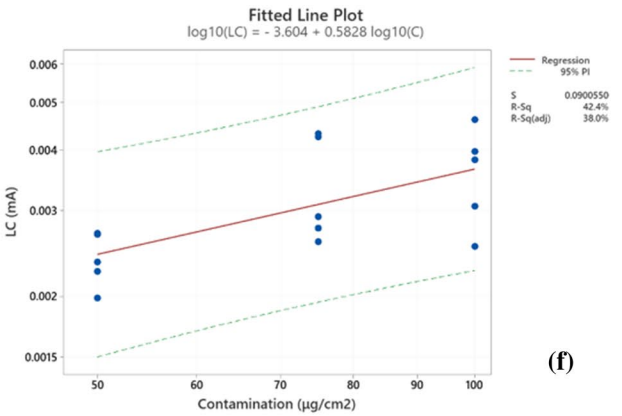
Fitted Line Plot
log10(LC) = - 3.604 + 0.5828 log10(C)
Regression
95% PI
S 0.0900550
R-Sq 42.4%
R-Sq(adj) 38.0%
LC (mA)
Contamination (µg/cm2)

(f)

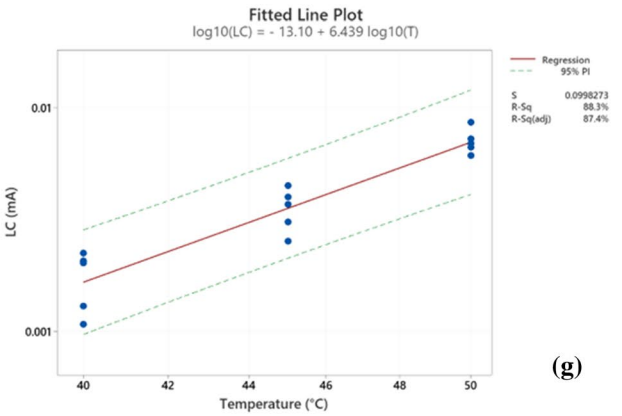
Fitted Line Plot
log10(LC) = - 13.10 + 6.439 log10(T)
Regression
95% PI
S 0.0998273
R-Sq 88.3%
R-Sq(adj) 87.4%
LC (mA)
Temperature (°C)

(g)

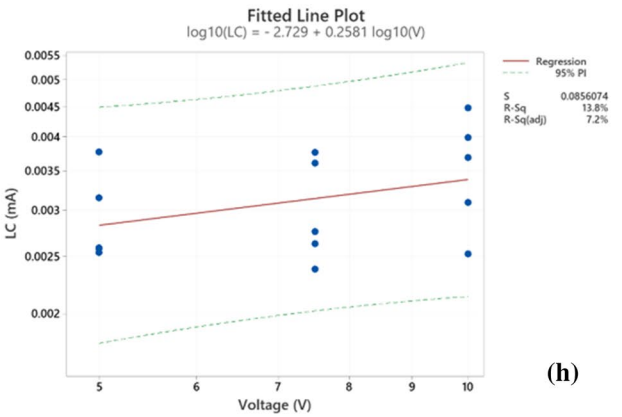
Fitted Line Plot
log10(LC) = - 2.729 + 0.2581 log10(V)
Regression
95% PI
S 0.0856074
R-Sq 13.8%
R-Sq(adj) 7.2%
LC (mA)
Voltage (V)

(h)

◂**Fig. 4** The TTF values versus three levels of each factor, along with the fitted line plot, prediction interval (PI), and regression equation on their trends at the same experimental condition for four critical factors including (a) Pitch distance, (b) Contamination, (c) Temperature, (d) Voltage. In addition, The LC values versus three levels of each factor, along with the fitted line plot, prediction interval (PI), and regression equation on their trends at the same experimental condition for four critical factors including (e) Pitch distance, (f) Contamination, (g) Temperature, (h) Voltage.

## Results and Discussion

### LC and TTF Study for Each Factor

The behavior of two responses (i.e., LC and TTF from Fig. 2) in three levels of each factor (vertical columns of Table I), along with the fitted line plot, prediction interval (PI), and regression equation on their trends is exhibited in Fig. 4. The figure clearly shows the effect of increasing pitch distance and decreasing other factors for TTF response and inverse behavior for LC response. All the experiments were conducted in a constant condition with a combination of the medium level of pitch distance and temperature factors and the high level of contamination and voltage factors (P2, C3, T2, V3) according to Table I.

By approximately doubling the pitch distance (from P1 to P2), TTF increases about sevenfold (or reducing pitch distance from P2 to P1, TTF shows a sevenfold decrease). However, by doubling the values of voltage (from V1 to V3) the average of TTF decreases about 1.5-fold. Interestingly, an increase of contamination level (from C1 to C3) showed only a small change in failure time compared to other parameters. Temperature, on the other hand, showed an 8.5-fold decrease in TTF for a change of temperature from T1–T3. The regression equations (shown above the graphs) on TTF trends for each factor at the same experimental condition can be used for forecasting the approximate failure time.

Figure 5 shows the comparison of the average of two responses in three levels of each factor, as an overview. Generally, the TTF decreases by increasing the LC with respect of various parameters because increasing LC represents more dissolution of metallic ions (in this case, Sn ions), which will assist earlier ECM formation. As shown by Fig. 5, temperature clearly demonstrates a greater effect compared to other factors, which shows maximum change in LC and TTF. Following this, pitch distance showed a significant effect on TTF, while LC was not significantly affected. Voltage and contamination showed a lower effect on LC values, while voltage showed more of an effect on TTF.

Figure 6 illustrates the Weibull distribution parameters estimated in the Minitab statistical software using goodness-of-fit tests and the maximum likelihood method. Furthermore, it shows the probability density function (PDF) of four changeable factors that belong to four vertical columns of Table I with 2000 random number simulations. The TTF distribution of pitch distance and temperature effects represent high PoF in the initial time of experiments. However, TTF distribution of contamination and voltage show that high PoF is in around 7 h and 8 h, respectively. Table II presents the appropriate distribution using goodness-of-fit tests for the pitch distance factor. Similarly, goodness-of-fit tests have been checked for all other conditions to fit the proper distribution with their parameters at different risk values ($\alpha$).

The average of TTFs and LCs for each factor, as well as the PoF at four time periods (extremely fast, under 1 h; fast, between 1 h and 4 h; medium, between 4 h and 7 h; and slow, over 7 h) based on appropriate Weibull distribution is provided in Table III. The table presents the overall insight of the PoF of each factor in similar experimental conditions on PCB surfaces. Generally, pitch distance, temperature, contamination, and voltage with three levels of measurement in this study have the highest risk of creating failure on the PCB surface, respectively. Among the individual parameters, pitch distance and temperature showed more significant effect compared to contamination and voltage. Although the contamination effect is temperature dependant, a greater effect of pitch distance and temperature shows the increasing reliability issues connected to the miniaturization and use of electronics in varying climatic conditions exposing them to different temperatures.[13,46]

### Investigation of Vertical Experimental Conditions

In order to simplify the experimental conditions for analysis, two categories of conditions (vertical and horizontal parts) have been defined. SIR measurements of three levels of each factor in conditions (P2, C3, T2, V3, and adipic acid as the only contamination at 98% RH for the chosen duration of 20 h) have been conducted at nine different experimental conditions in the vertical part of Table I. For example, in the vertical part in the second column of Table I, the three different conditions are explained, considering just pitch distance as variable at a fixed condition (C3, T2, V3). Table IV lists the Weibull distribution parameters for the TTF data for all factors/levels, along with the PoF on four time periods (highly fast, fast, medium, and slow) in vertical experimental conditions. This table presents the numerical average values of TTF and LC based on five replication experiments, in addition to Weibull parameters and PoF in the four time periods of each experimental condition. The P1A100C45V10 and P2a100c50v10 conditions display the highest PoF in all time periods. Small pitch distance (P1) in the first condition and highest temperature (T3) in the second condition have a key role in making a risk condition on the PCB surface. Compared to Table III, Table IV presents the details of all factor levels instead of each factor. Figure 7 shows the PDF of the Weibull distribution for three levels of each factor. It

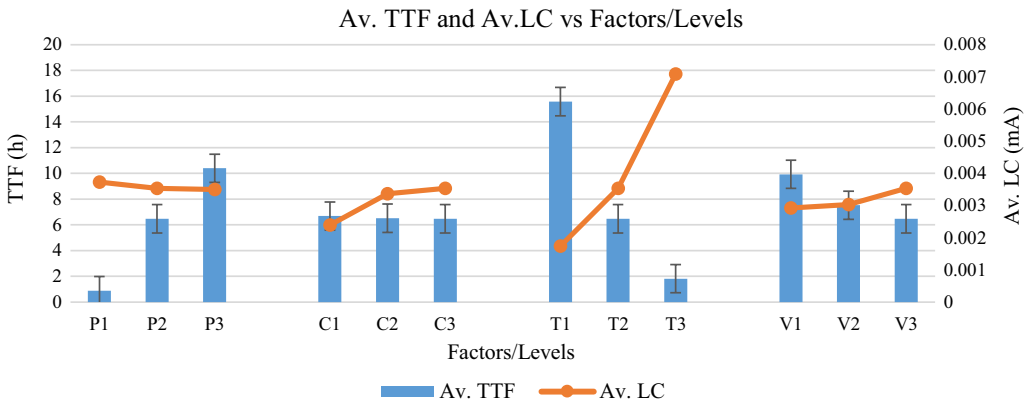


**Fig. 5** The comparison of the average of two responses in three levels of each factor.

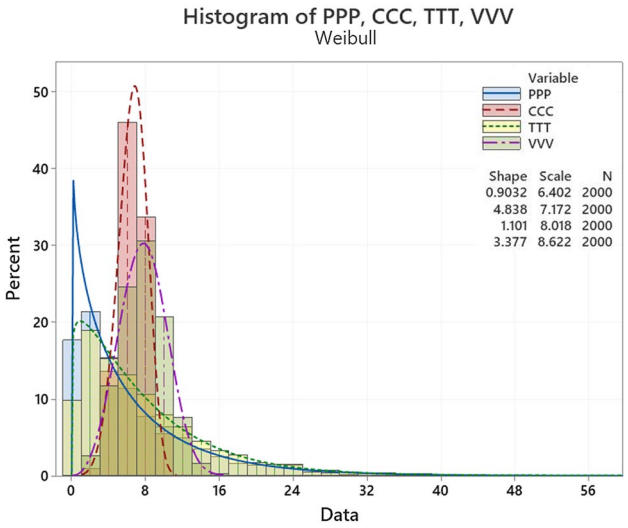


**Fig. 6** Probability density function (PDF) of TTF for four critical factors.

visually displays the probability behavior of TTF data for each condition over time.

The average TTF at similar conditions increased from P1 to P3. However, the LC values represent a uniform behavior with an extremely low and negative movement from P1 to P3. The Weibull distribution for TTF estimates that P1 has a high risk, especially in a fast failure class with a probability rate of about 70%.

The effect of three contamination levels (C1, C2, C3) of one WOA type on TTF and LC has provided the decreasing and an ascending trend from the low to the high level, respectively. The high level of contamination has the greatest, but not severe, effect on TTF and LC because there is more water adsorption by the high level of contamination (C3), which increases surface electrochemical activity (conductivity) by the dissolution of the metal ions on the PCB surface. The PoF in C3 also presents a high value, especially

**Table II** The goodness-of-fit test summary for pitch distance factor

| Weibull distribution | | | | | |
|---|---|---|---|---|---|
| *Kolmogorov–Smirnov* | | | | | |
| Sample size | | | 2000 | | |
| Statistic | | | 0.01667 | | |
| *P*-value | | | 0.62853 | | |
| α | 0.2 | 0.1 | 0.05 | 0.02 | 0.01 |
| | 0.0239 | 0.0273 | 0.0303 | 0.0339 | 0.0364 |
| Critical value | 9 | 5 | 7 | 4 | 3 |
| Reject | No | No | No | No | No |
| *Anderson–Darling* | | | | | |
| Sample size | | | 2000 | | |
| Statistic | | | 0.38585 | | |
| α | 0.2 | 0.1 | 0.05 | 0.02 | 0.01 |
| Critical value | 1.3749 | 1.9286 | 2.5018 | 3.2892 | 3.9074 |
| Reject | No | No | No | No | No |
| *Chi-squared* | | | | | |
| Deg. of freedom | | | 10 | | |
| Statistic | | | 5.8576 | | |
| *P*-value | | | 0.82708 | | |
| α | 0.2 | 0.1 | 0.05 | 0.02 | 0.01 |
| Critical value | 13.442 | 15.987 | 18.307 | 21.161 | 23.209 |
| Reject | No | No | No | No | No |

in the initial hours of experiments compared to other levels (C1, and C2).

The three levels of temperature factor at T1, T2, and T3 are shown a completely different range of TTFs and LCs. Temperature is the only factor that significantly affects the behavior of LC at all levels, since LC increased about twofold from T1 to T2 and increased fourfold from T1 to T3. The effect of T3 for creating the failure is about two times and 15 times higher than T2 and T1, respectively. The PoF

**Table III** The PoF summary of critical factors at four hypothetical periods of time

| Factors | Symbol | Av. TTF (h) | Av. LC (mA) | PoF under 1 h (%) | PoF under 4 h (%) | PoF under 7 h (%) |
|---|---|---|---|---|---|---|
| Pitch distance | P | 5.92 | 0.003588 | 17 | 48 | 66 |
| Contamination | C | 6.53 | 0.003117 | 0 | 5 | 58 |
| Temperature | T | 7.98 | 0.004127 | 10 | 37 | 59 |
| Voltage | V | 8.00 | 0.003170 | 0 | 7 | 39 |

*TTF* Time to failure, *LC* Leakage current.

in T3 also presents a high value compared to the other levels of temperature.

V1, V2, and V3 are considered low, medium, and high levels of the voltage factor. The effect of V3 is higher than other levels. In other words, with increasing the voltage level (from V1 to V3) at the same conditions, about 3 h on TTF and about 0.6 µA on LC, changes are obvious. Generally, voltage similar to contamination follows a significant shallow effect on responses. The PoF results especially show the effect of high level compared to low level of voltage in the last assumed time period (under 7 h).

## Investigation of Horizontal Experimental Conditions

In the horizontal part, three other conditions with low, medium, and high levels of each factor together, have been investigated. Table V provides the average of TTFs and LCs of three different conditions at low, medium, and high levels of the horizontal part of Table I, as well as their probability distribution parameters and probability of failure for each time period that is assumed. It can be concluded from the percentages that the combination of the low levels of each factor has the highest risk rather than other conditions. It can be understood that pitch distance has a significant effect in the probability of failure as mentioned before. As seen from the vertical conditions, by increasing V, T, and C and decreasing P, the PoF is increased. The conclusion from the horizontal condition confirms the latter conclusion from the vertical condition. However, the horizontal conditions display the important effect of pitch distance factor, which by increasing the other parameters except for P, the PoF decreases and the P3a100c50v10 condition has the lowest PoF and the P1a50c40v5 condition has the highest risk.

Figure 8a and b depicts the comparison of the LC average and average of TTF versus three different levels of all factors together, as well as the Weibull probability density distribution of TTF versus time data for all low, medium, and high levels of four changeable factors, respectively. Both TTF and LC demonstrate an increasing trend from a low level to a high level. However, the average range of LC change from low to high is higher compared to TTF. Row 3 (high level combination of each factor) from the distribution plot, exhibits denser TTF data in comparison with other levels, representing the TTF data set with more density and lower scattering in this condition.

## Comparison of Pitch Distance and Temperature as Two Significant Factors

According to the results of vertical and horizontal experimental conditions, the pitch distance and temperature factors are more significant than other parameters. Therefore, one more experimental condition has been considered for each to obtain the best understanding of these two factor effects. For pitch distance at similar contamination and voltage levels (C3, V3) and only changing the temperature levels to T3 (50°C), LC and TTF of three different levels of pitch distance have been measured. Furthermore, the average of LC and TTF of three temperature levels on smaller pitch distance (P1) and similar contamination and voltage levels (C3, V3) at 98% RH with adipic acid for 20 h have been examined.

The average of TTF and LC values of three levels of pitch distance at two different temperatures (i.e., P1C3T2V3, P2C3T2V3, P3C3T2V3 and P1C3T3V3, P2C3T3V3, P3C3T3V3 conditions) are shown in Fig. 9. However, the TTF trend at both temperatures from P1 to P3 follows an increasing tendency while at the high temperature level (50°C), the average TTF at each pitch distance is lower than the low temperature level (45°C). This difference is more than 40, 280, and 160 min for P1, P2, and P3, respectively.

The small pitch distance demonstrates the very fast class (under 1 h) of failure time at both temperatures. In addition, the large pitch distance at both temperatures shows the low class (above 7 h) of TTF. The LC trends for both temperatures also show the same decreasing behavior from P1 to P3. For P3, there is more scatter in the result of TTF contrary to the P1 experiment owing to a large distance between the two electrodes; therefore, dynamic formation of water film and connection between both electrodes are more random.

Figure 10 illustrates the average comparison of TTF and LC for the temperature at three levels by two different pitch distances. The TTFs of both pitches simultaneously follow a similar decreasing trend while LCs follow an increasing trend. The difference of TTFs for T1, T2, and T3 at P2 is about 1.5 h more than P1. TTF reduction intensity from T1

**Table IV** The probability distribution parameters and the probability of failure for each level of each factor at 12 vertical conditions

| Experimental conditions | Symbol | Av. TTF (h) | Av. LC (mA) | Fitted distribution by 2000 simulations | $\beta$ | $\alpha$ | $\theta$ | PoF under 1 h (%) | PoF under 4 h (%) | PoF under 7 h (%) |
|---|---|---|---|---|---|---|---|---|---|---|
| P1A100C45V10 | P1 | 0.89 | 0.00373 | Weibull (3P) | 0.77440 | 0.30216 | 0.63001 | 69 | 99 | 100 |
| P2A100C45V10 | P2 | 6.47 | 0.00354 | Weibull (3P) | 2.45100 | 6.51270 | 0.07488 | 1 | 25 | 69 |
| P3A100C45V10 | P3 | 10.40 | 0.00350 | Weibull (3P) | 3.84270 | 10.02800 | 0.62985 | 0 | 1 | 16 |
| P2a50c45v10 | C1 | 6.68 | 0.00239 | Weibull (3P) | 8.18240 | 7.53340 | − 0.78882 | 0 | 2 | 73 |
| P2a75c45v10 | C2 | 6.52 | 0.00336 | Weibull (3P) | 3.59300 | 6.33070 | 0.43679 | 0 | 12 | 68 |
| P2a100c45v10 | C3 | 6.47 | 0.00354 | Weibull (3P) | 2.45100 | 6.51270 | 0.07488 | 1 | 25 | 69 |
| P2a100c40v10 | T1 | 15.57 | 0.00174 | Weibull (3P) | 4.31580 | 17.04700 | − 0.94876 | 0 | 0 | 4 |
| P2a100c45v10 | T2 | 6.47 | 0.00354 | Weibull (3P) | 2.45100 | 6.51270 | 0.07488 | 1 | 25 | 69 |
| P2a100c50v10 | T3 | 1.82 | 0.00709 | Weibull | 3.70360 | 1.72750 | 0 | 12 | 100 | 100 |
| P2a100c45v5 | V1 | 9.92 | 0.00293 | Weibull | 42.2590 | 9.65760 | 0 | 0 | 0 | 0 |
| P2a100c45v7.5 | V2 | 7.53 | 0.00303 | Weibull (3P) | 6.40520 | 8.79980 | − 1.23850 | 0 | 3 | 48 |
| P2a100c45v10 | V3 | 6.47 | 0.00354 | Weibull (3P) | 2.45100 | 6.51270 | 0.07488 | 1 | 25 | 69 |

to T3 for P2 is greater in comparison with P1. However, increasing LC intensity from T1 to T3 for P1 is higher compared to P2, especially at the high temperature level (T3).

## CART and Multivariate Regression Analysis

The classification tree using the Gini method in Minitab statistical software as a splitting method is applied to gain the best group split into 70 TTFs of all experiments. This tree considers all multinomial predictors (i.e., pitch distance, contamination, temperature, and voltage) at each node, and the calculation for the split improvement amount, results in predicted probabilities for terminal nodes at four classes (i.e., highly fast, fast, medium, and low). The validation of the classification model has been performed by the k-fold cross-validation method, which is one of the most widely used methods for model validation.[47,48] The 10-fold cross-validation is used to estimate the model performance in prediction. The area under the receiver operating characteristic (ROC) curve (AUC) is an important metric to distinguish the model's performance.[49] ROC is a probability curve, which graphically shows the trade-off between true positive rate (sensitivity) and false positive rate (specificity).[50] The AUC of the average of all classes is 0.93, which indicates good classification performance for prediction. Table VI exhibits the details of the 10-fold cross-validation method by minimum misclassification tree criteria in training and testing the data set. The nine optimal nodes by minimum misclassification criteria are estimated for all TTF data and are presented in Fig. 11. The node split view of the classification tree (lower left side of Fig. 11) presents the condensed view of factor effects to create separate classes. For instance, the most probability of failure (90%) in the highly fast situation (under 1 h, green) belongs to the terminal node 3, which follows only two factors of pitch distance of less than 450 µm and a temperature higher than 42.5°C.

The regression tree is employed to visualize and identify the most important predictors and discover combinations of predictor settings that are most likely to lead to a lower or higher TTF. Figure 12 shows a regression tree diagram with seven optimal nodes selected by maximun $R^2$ criteria. Similar to the classification tree, the regression tree works by splitting the TTF data into divisions based on the predictor settings that best separate the data into identical TTF values.

Figure 13 displays the ANOVA table of the reduced model on TTF response using the stepwise backward elimination method and the residual plot for the TTF data set that presents the normality of residual data and constant variance without following a specific trend to emphasize the adequacy of the model. Additionally, the regression equation presented below can predict the TTF value based on four critical factors. According to the table, pitch distance, temperature, voltage, and contamination are the most significant effects.

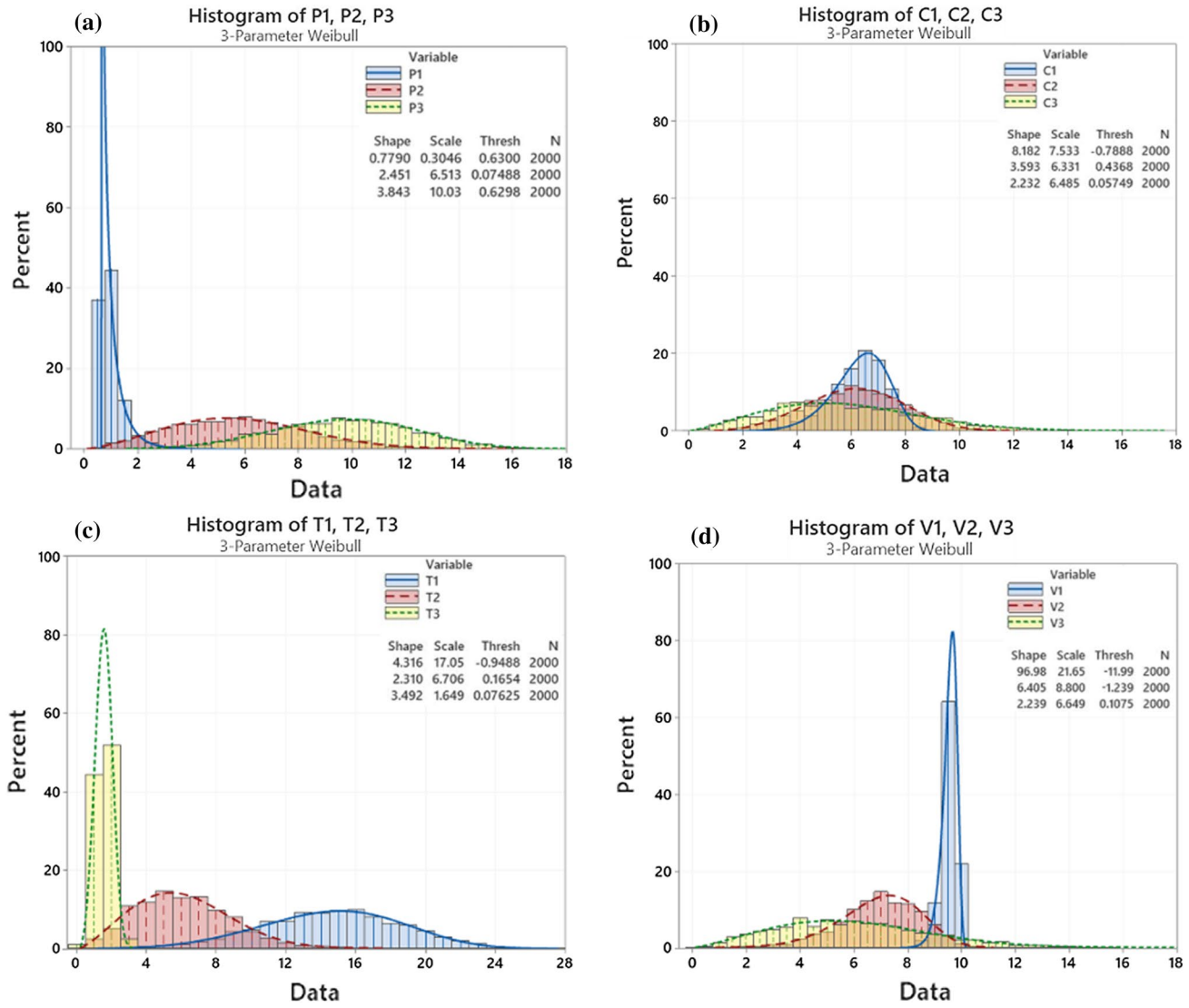


**Fig. 7** The probability failure distribution plot for three levels of four critical factors including (a) Pitch distance, (b) Contamination, (c) Temperature, (d) Voltage.

Similar to the multivariate regression model on TTF response, another regression analysis has been performed on the Weibull distribution parameters estimated for each condition as a specific novelty in this study. This means a regression analysis is used to estimate the critical factor effects on probabilistic distribution parameters. There are no significant terms for $\gamma$, and the regression equation of the probabilistic distribution parameters is made only from $\alpha$ and $\beta$.

## Model Validation and Interpretation

The validation of three regression models has been performed by the k-fold cross-validation method. This method is commonly used for model validation and model selection.[51] Table VII summarizes of the regression models with the determination coefficient ($R^2$) and the standard deviation of the error between the model and experiment on the TTF data set with 10-fold cross-validation. $R^2$ is the percentage of variation in the response that the model shows, and close to 1 demonstrates how well the data are fitted in the regression model.[52,53] The table also includes $R^2$ for the training and testing of the TTF data set. The $R^2$ test usually gives a better scale of how the model works for the prediction.[54]

To examine the model's accuracy, a specific condition (600 µm pitch distance, 60 µg/cm$^2$ contamination, 46°C, and 6 V) has been investigated. The TTF predicted values of (b) the classification tree, (c) the regression tree, (d)

**Table V** The probability distribution parameters and the probability of failure for each condition at the horizontal part

| Experimental conditions | | Av. TTF (h) | Av. LC (mA) | Fitted distribution by 2000 random numbers | $\beta$ | $\alpha$ | $\theta$ | Probability of failure under 1 h (%) | Probability of failure under 4 h (%) | Probability of failure under 7 h (%) |
|---|---|---|---|---|---|---|---|---|---|---|
| P1a50c40v5 | Row1 | 7.01 | 0.000910 | Weibull (3P) | 2.9739 | 7.0491 | 0.05538 | 0 | 16 | 62 |
| P2a75c45v7.5 | Row2 | 8.06 | 0.002324 | Weibull (3P) | 3.0708 | 8.4768 | − 0.32717 | 0 | 12 | 47 |
| P3a100c50v10 | Row3 | 8.26 | 0.004616 | Weibull (3P) | 7.6177 | 7.1307 | 0.83666 | 0 | 0 | 28 |

the multivariate regression analysis, and (e) the probabilistic distribution regression models, have been calculated to compare with (a) experimental data of five replications. Table VIII compares the accurate prediction of each model, as well as their comparison with five experimental results of TTFs at the instance condition. The prediction interval (PI) is a range that is likely to contain a single future response, and it is used to assess the precision of the predictions.

All the prediction models can correctly forecast the TTF of all conditions between the lower and upper PIs. The probabilistic distribution regression model was employed for the probability of TTF estimation. It has straightforward interpretation; however, it was challenging to fit applicable distribution in some data sets and had the lowest $R^2$ compared to the other regression models. The regression tree model with 65% $R^2$ test was utilized for visual and fast decisions. It had acceptable accuracy with standard deviation variation, which needs more data for its training part for more precision. Generally, these models can be selected for each case study according to the dataset, accuracy, and prediction limit at various conditions. Nevertheless, the multivariate regression model had the best prediction with the highest $R^2$ test (84%) and lowest test error value (0.45) for the TTF data set.

## Perspectives on Modelling Result in Relation to Humidity Effects on Electronics

Given that there are various conditions (combination of different factors and levels) that affect TTF due to ECM, different approaches such as probabilistic distribution analysis, multivariate regression analysis, and CART analysis have been studied to predict the probability of TTF and failure risk prediction on the PCB surface. Comparing with literature information on the effect of various parameters on humidity robustness of electronics[55–58] The models described in this paper are based on the combinations of three levels of four critical factors showing the prediction of time-to-failure due to ECM on a PCB surface. Moreover, these statistical, probabilistic, and machine learning methods have been selected based on the probabilistic predictive analytics framework.[59] Therefore, finding the best approach and prediction model can give a better perception of PCB reliability, which can be used for preventive measures.

This study has also evaluated the predictive modelling of TTF and demonstrates that the TTF distribution using Weibull provides a better understanding of critical conditions for having the best TTF probability prediction based on the results in this paper. The Weibull distribution has been utilized in probabilistic analysis since it is most widely used to predict life and failure data sets under multiparameter influence. Table IX displays the effect of each factor in creating different TTF prediction models. The percentage influence of pitch distance and temperature in all predictive

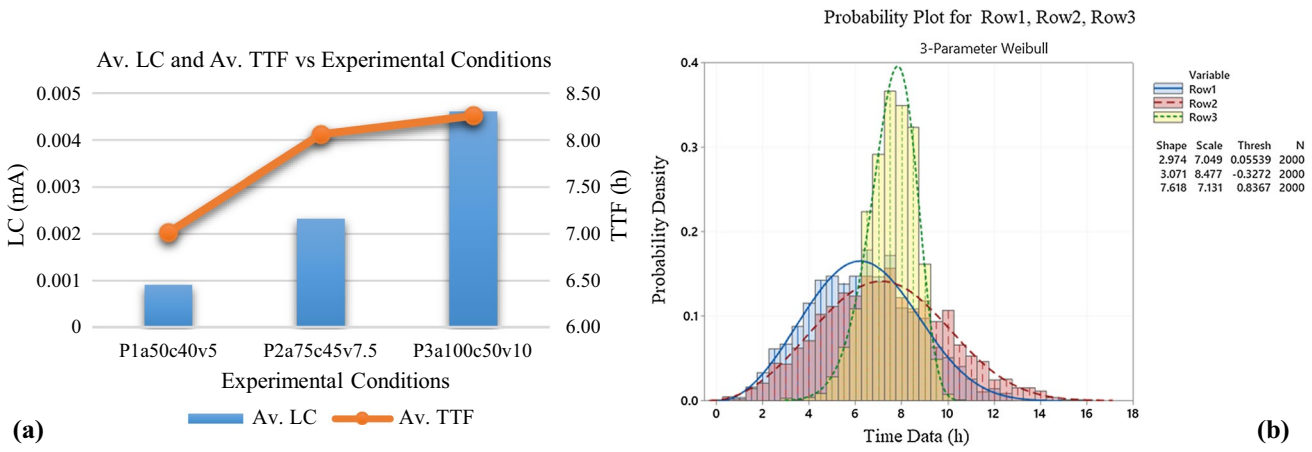


**Fig. 8** (a) The average comparison of the LC and TTF versus three different levels of all factors together. (b) The probability distribution of failure for three levels of four changeable factors in horizontal part.

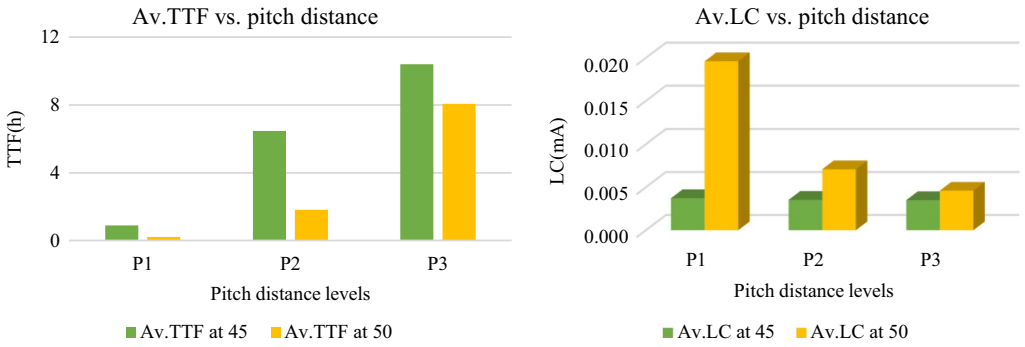


**Fig. 9** The average TTF and LC values of three levels of pitch distance at two different temperatures.

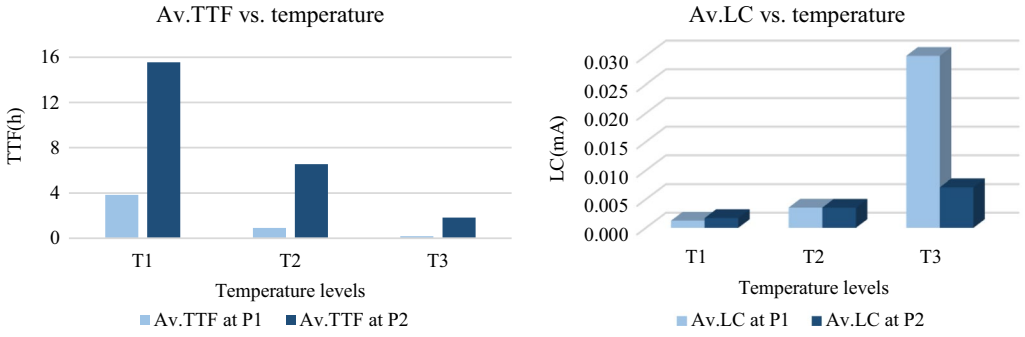


**Fig. 10** The comparison of two different temperature conditions.

models is more remarkable than the effect of contamination and voltage factors.

### Effect of Pitch Distance and Temperature

The effect of the factors concerning the humidity effects are clearly visible in the classification and regression tree (Figs. 11 and 12), as well as ANOVA table (Fig. 13). The classification and regression tree illustrates pitch distance and temperature as significant factors since they present the pitch distance and temperature as the initial splitters in the top of the trees, which define how the nodes can be partitioned. Moreover, the contribution percentage of pitch distance and temperature on the multivariate regression model

**Table VI** Model validation by minimum misclassification tree criteria

| | Classification tree (10-fold cross-validation and minimum misclassification criteria) |
|---|---|
| Node | 9 |
| AUC | 0.93 |
| Misclassification rate (Training) | 0.23 |
| Misclassification rate (Test) | 0.39 |

in the ANOVA table show the great effect of these factors compared to the contamination and voltage. The pitch distance is a significant factor in relation to the humidity effect on electronics failure, which is reduced considerably due to constant electronic miniaturization for reducing the space of PCB and high component density. The importance of pitch distance is due to increasing the electric field, thereby making it easy for dendrites to form during electrochemical migration.[60,61] The smaller pitch distance (P1) on the PCB surface can make an electrochemical cell easier due to water layer formation between two electrical points. According to

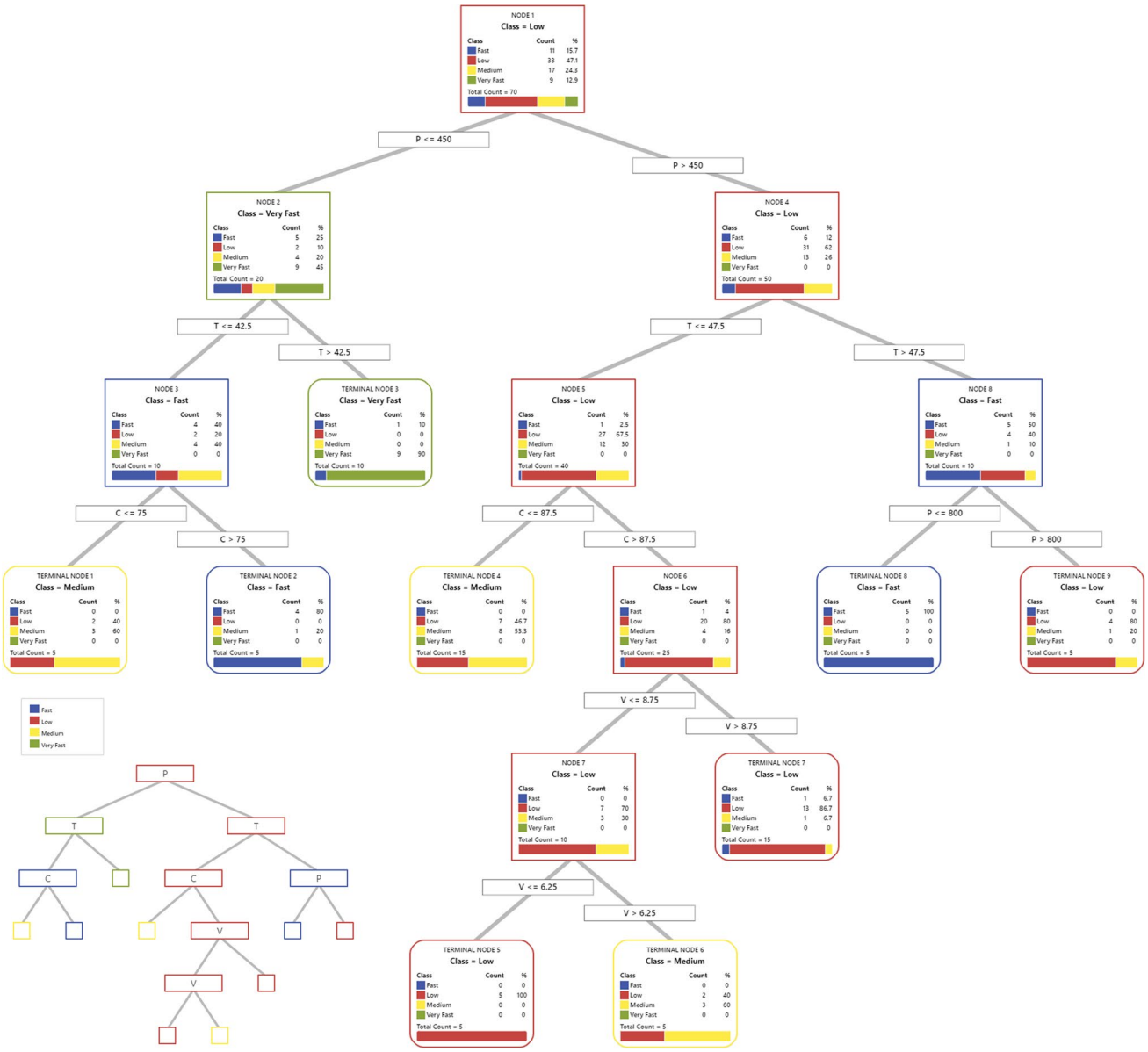


**Fig. 11** Classification tree diagram for TTF data with four predictors and classes provided.

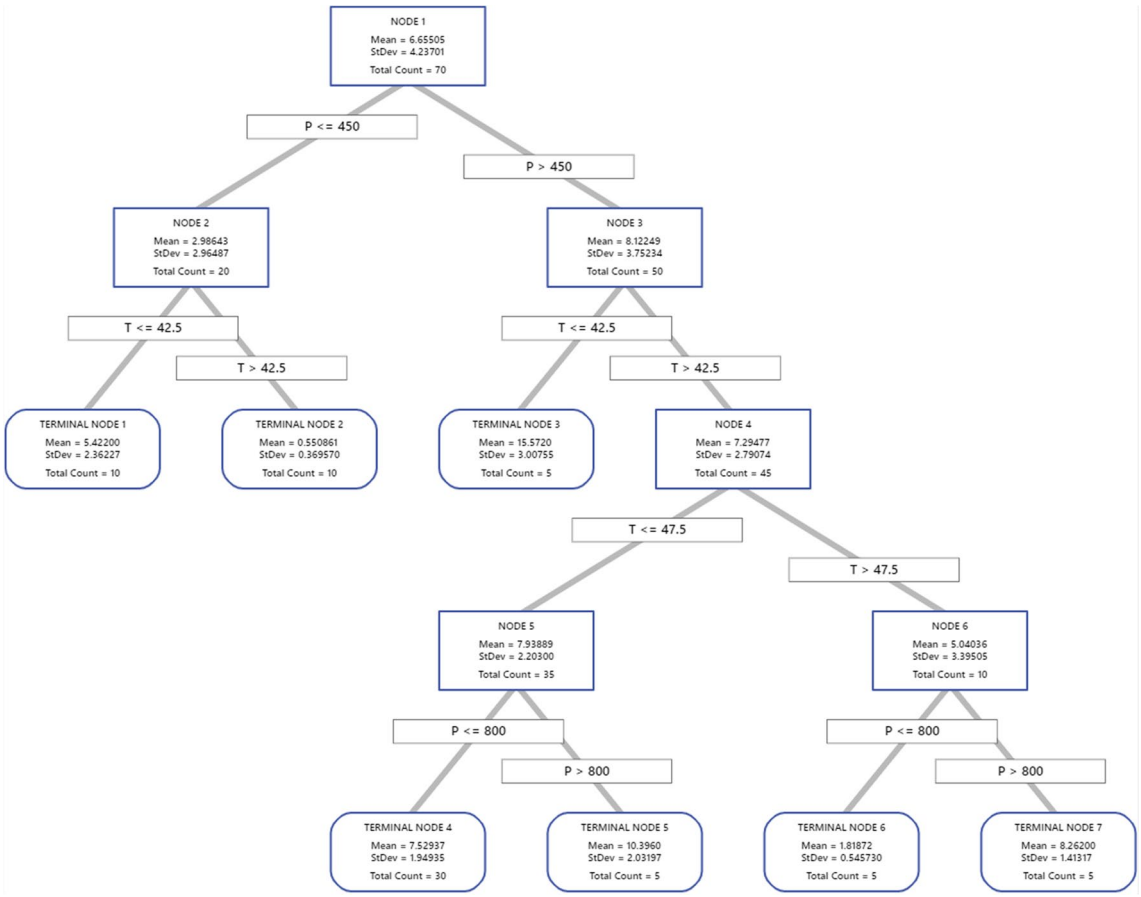


**Fig. 12** The optimal regression tree diagram for TTF response.

| *Source* | D F | SS | Contribution | MSS | F-value | P-value |
|---|---|---|---|---|---|---|
| Regression | 4 | 78.389 | 86.50% | 19.5973 | 104.12 | 0 |
| Pitch distance | 1 | 27.827 | 30.71% | 56.4091 | 299.71 | 0 |
| Contamination | 1 | 9.527 | 10.51% | 0.81 | 4.3 | 0.042 |
| Temperature | 1 | 37.165 | 41.01% | 31.4373 | 167.03 | 0 |
| Voltage | 1 | 3.871 | 4.27% | 3.8706 | 20.57 | 0 |
| Error | 65 | 12.234 | 13.50% | 0.1882 | | |
| Lack-of-Fit | 9 | 8.344 | 9.21% | 0.9271 | 13.35 | 0 |
| Pure Error | 56 | 3.89 | 4.29% | 0.0695 | | |
| Total | 69 | 90.623 | 100 % | | | |

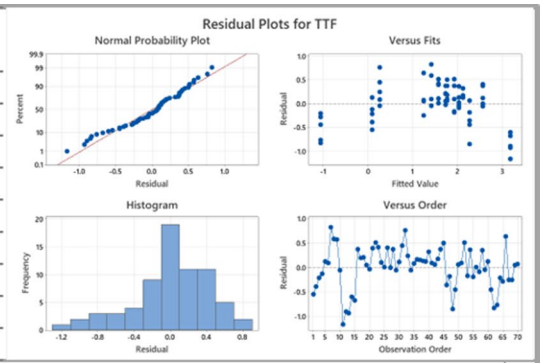


*ln(TTF)= 11.165 + 0.004418 Pitch distance - 0.00643 Contamination - 0.2301 Temperature - 0.1406 Voltage*

**Fig. 13** ANOVA table, residual plots, and regression model summary for the TTF data set.

the TTF data set, with every 100-µm pitch distance increase, approximately 1 h is added to the TTF. Temperature is found to be a significant factor in causing failure. Temperature can influence the humidity effects in different ways, namely, by (i) increasing the absolute humidity in the environment to interact with PCB surface, (ii) reducing the deliquescent humidity level for contamination and increasing its solubility, and (iii) increasing the kinetics of electrochemical process including the deposition process for ECM. For condensation, the dew point range and the size of dew droplets formed on the PCB surface are affected by temperature.[62,63]

### Effect of Contamination and Voltage

As shown in Fig. 3, Table IV, and modelling results, the contamination effect on TTF is not as significant as pitch distance and temperature. However, the effect of contamination should be considered together with temperature because when deliquescence occurs, a near saturated solution of contamination to the absorbed water forms, which remains saturated irrespective of the level of contamination unless the temperature is different. Therefore, although contamination on the surface of the PCB has changed, concentration in the water layer will not change significantly; hence, it should not influence the TTF significantly at constant temperature. The voltage in relation to humidity also has less of an effect on TTF, which might be due to the extent of current that can be passed through the limited thickness of the water layer. Therefore, an increase in voltage will not significantly influence the leakage current and SIR reduction for dissolving metal ions and forming dendrites on the PCB surface, unless other parameters such as P, T, or C change. However, after pitch distance and temperature, voltage also has a significant effect on TTF, and with a twofold increase, TTF decreases more than 3 h.

**Table VII** The comparison of three regression models

| | Multivariate regression model | Probabilistic distribution regression model | Regression Tree model |
|---|---|---|---|
| $R^2$ (training) | 87% | 64% | 80% |
| $R^2$ (test) | 84% | 59% | 65% |
| Error (training) | 0.43 | 0.56 | 0.37 |
| Error (test) | 0.45 | 0.58 | 0.51 |

### Combined Effect of Pitch Distance, Contamination, and Temperature

The interaction between all three factors together with voltage effect is indirectly linked to the pitch distance, and temperature plays a big role in enhancing the effect of pitch distance and temperature due to the factors mentioned above. Kamila et al.[64–66] reported that the hygroscopic nature of residues is determined by the chemistry of the activating part

**Table VIII** The comparison of TTF predictor models together is based on five experimental results of one specific condition

| Prediction models | Note | Fitted Value | Lower PI | Upper PI |
|---|---|---|---|---|
| a. Experimental data of five replications | 5.84 | 7.32 | 5.58 | 9.96 |
| | 7.09 | | | |
| | 8.12 | | | |
| | 5.58 | | | |
| | 9.96 | | | |
| b. Classification tree | Terminal node ID=3 (Medium class) | 53% probability of medium class and 47% probability of low class | 0% | 100% |
| c. Regression tree | Terminal node ID=4 | 7.53 | 5.58 | 9.48 |
| d. Multivariate regression | | 7.4 | 2.99 | 18.28 |
| e. Probabilistic distribution regression | Weibull distribution with these parameters: α=8.98151, β=8.20630 | With 95% probability, all of the TTFs in this condition occur in a 10.27-h period | | |

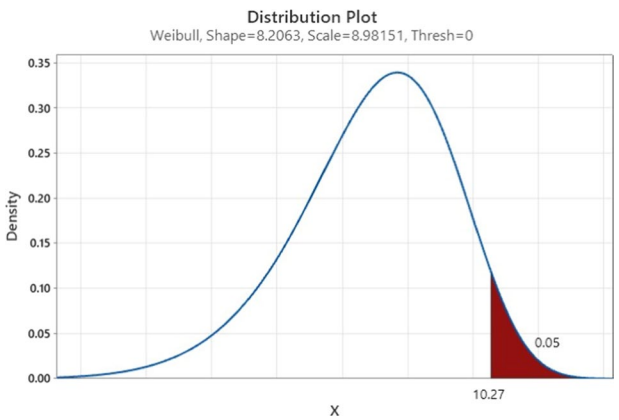

**Table IX** The percentage of factors effects on each TTF prediction model

| | Multivariate regression model (%) | Probabilistic distribution regression model (%) | Regression tree model (%) | Classification tree model (%) |
|---|---|---|---|---|
| Pitch distance | 46 | 47 | 39 | 31 |
| Temperature | 35 | 26 | 44 | 28 |
| Contamination | 13 | 21 | 9 | 23 |
| Voltage | 6 | 6 | 8 | 18 |

of flux formation and temperature. An increase of temperature strengthens the interaction between the acid and water vapor, leading to high uptake of moisture by flux residues. An increase of temperature shifts the critical relative humidity level for deliquescence of flux activators towards lower RH range, and the solubility of the residues increases. At higher ambient temperatures, the formation of a conductive electrolyte is accelerated, and an increase in LC and subsequent electrochemical metal ion migration occur at lower RH levels.

## Conclusion

- The consensus of characterizing the critical factors/levels, probability of failure, and failure time prediction modeling give extensive insight into the failure occurrence on PCB surfaces under humidity.
- Statistically, the temperature and pitch distance had the most significant effect on TTFs, respectively. They were especially significant in the risk of failure period of the very fast and fast classes.
- The importance of pitch distance in significantly decreasing TTF is due to increasing the electric field to make dendrite formation easier during electrochemical migration. In addition, the importance of temperature in TTF is because of the influence on humidity to alter the dew point range and the size of dew droplets form on the PCB surface, as well as increasing the electrochemical kinetics.
- Results indicated that with every 100-µm increase in pitch distance, TTF is increased by approximately 80 min. Moreover, it also increased around 80 min by every 1°C decrease in temperature. Nevertheless, every 1 V increase added about 40 min to the TTF, and for every 10 µg/cm$^2$ increase of contamination level, TTF only showed around a 2.5-min increase.
- The high temperature and large pitch distance rather than voltage and contamination factors also had the strongest effect on the LCs. Additionally, the combination of small pitch distance (P1) and the high temperature level (T3) displayed a critical condition with the highest LC value and failure probability percentage compared to other conditions.
- The classification tree was used for the qualitative estimation of TTFs for a different period, which shows a satisfactory probability prediction of the periods and gives an excellent and quick insight into the data set. For instance, the very fast class, which shows the critical conditions with failure occurring in under 1 h (TTF< 1 h), is due to conditions of low pitch distances and high temperatures (P < 450 µm and T> 42.5°C).
- From all regression models, the multivariate regression analysis analyzing the statistical significance of factor effects and determining their correlation had the best validation and prediction with the close value to real data, highest $R^2$, and lowest error.

**Acknowledgments** The present research work was carried out as a part of work in CELCORR/CreCon Consortium (https://celcorr.dtu.dk). The authors would like to acknowledge the CELCORR/CreCon Consortium and Innovation Fund Denmark for the funding support.

**Conflict of interest** The authors declare that they have no conflict of interest.

## References

1. R. Ambat, H. Conseil-Gudla, and V. Verdingovas, Corrosion in Electronics, *Encycl. Interfacial Chem. Surf. Sci. Electrochem.* 134 (2018).
2. J. Sjoberg, D. A. Geiger, and D. Shangguan, Process Development and Reliability Evaluation for Inline Package-on-Package (pop) Assembly, *Electron. Components Technol. Conf. IEEE.* 2005 (2008).
3. K. Vijay, Miniaturization - Solder Paste Attributes for Maximizing the Print & Reflow Manufacturing Process Window, *Electron. Syst. Technol. Conf. IEEE.* 1 (2012).
4. K. Piotrowska, M. S. Jellesen, and R. Ambat, Water Film Formation on the PCBA Surface and Failure Occurrence in Electronics, *Nord. Conf. Microelectron. Packag. IEEE.* 72 (2018).
5. J. Niemann, S. Härter, C. Kästle, and J. Franke, Challenges of the Miniaturization in the Electronics Production on the example of 01005 Components, *Kongresses Montage Handhabung Industrieroboter. Springer*. 113 (2017).
6. E. Guene, Solderability and Reliability Evolution of no Clean Solder Fluxes for Selective Soldering, *Eur. Microelectron. Packag. Conf. IEEE.* 1 (2017).
7. M. Judd and K. Brindley, *Soldering in Electronics Assembly* (Elsevier, 1992).

8. K. S. Hansen, M. S. Jellesen, P. Moller, P. J. S. Westermann, and R. Ambat, Effect of Solder Flux Residues on Corrosion of Electronics, *Annu. Reliab. Maintainab. Symp. IEEE.* 502 (2009).
9. Y. Gao, S.B. Chen, and L.E. Yu, Efflorescence Relative Humidity for Ammonium Sulfate Particles. *J. Phys. Chem. A* 110, 7602 (2006).
10. M.S. Jellesen, D. Minzari, U. Rathinavelu, P. Moller, and R. Ambat, Corrosion in Electronics at Device Level. *ECS Trans.* 25, 1 (2019).
11. J. Romero, M.H. Azarian, C. Morillo, and M. Pecht, Effects of Moisture and Temperature on Membrane Switches in Laptop Keyboards. *IEEE Trans. Device Mater. Reliab.* 18, 535 (2018).
12. H. Conseil-Gudla, Z. Staliulionis, S. Mohanty, M.S. Jellesen, J.H. Hattel, and R. Ambat, Humidity build-up in Electronic Enclosures Exposed to Different Geographical Locations by RC Modelling and Reliability Prediction. *Microelectron. Reliab.* 82, 136 (2018).
13. K. Piotrowska, M. Grzelak, and R. Ambat, No-clean Solder Flux Chemistry and Temperature Effects on Humidity-Related Reliability of Electronics. *J. Electron. Mater.* 48, 1207 (2019).
14. V. Verdingovas, S. Joshy, M. Stendahl Jellesen, and R. Ambat, Analysis of Surface Insulation Resistance Related Failures in Electronics by Circuit Simulation. *Circuit World.* 43, 45 (2017).
15. V. Verdingovas, M.S. Jellesen, and R. Ambat, Effect of Pulsed Voltage on Electrochemical Migration of Tin in Electronics. *J. Mater. Sci. Mater. Electron.* 26, 7997 (2015).
16. H. Conseil, M. Stendahl Jellesen, and R. Ambat, Contamination Profile on Typical Printed Circuit Board Assemblies versus Soldering Process. *Solder. Surf. Mt. Technol.* 26, 194 (2014).
17. C.H. Liao, S.H. Yang, M.Y. Liao, K.C. Chung, N. Kumari, K.H. Chen, Y.H. Lin, S.R. Lin, T.Y. Tsai, and Y.Z. Juang, A 23.6ppm/°C Monolithically Integrated GaN Reference Voltage Design with Temperature Range from – 50 °C to 200 °C and Supply Voltage Range from 3.9 to 24V, *IEEE Int. Solid-State Circuits Conf.* 72 (2020).
18. J.Y. Li, C.X. Sun, and S.A. Sebo, Humidity and Contamination Severity Impact on the Leakage Currents of Porcelain Insulators. *IET Gener. Transm. Distrib.* 5, 19 (2011).
19. K. Piotrowska, F. Li, and R. Ambat, Thermal Decomposition of Binary Mixtures of Organic Activators Used in no-Clean Fluxes and Impact on PCBA Corrosion Reliability. *Solder. Surf. Mt. Technol.* 32, 93 (2020).
20. V. Verdingovas, M.S. Jellesen, and R. Ambat, Solder Flux Residues and Humidity-Related Failures in Electronics: Relative Effects of Weak Organic Acids Used in No-Clean Flux Systems. *J. Electron. Mater.* 44, 1116 (2015).
21. V. Verdingovas, M.S. Jellesen, and R. Ambat, Relative Effect of Solder Flux Chemistry on the Humidity Related Failures in Electronics. *Solder. Surf. Mt. Technol.* 27, 146 (2015).
22. T. Zheng, Z. Wang, C. Tan, and R. Wang, Research on Fault Prediction and Diagnosis Method of PCB Circuit, *Int. Conf. Artif. Intell. Comput. Eng. IEEE.* 387 (2020).
23. Z. Zhang and F. Gong, Prediction and Analyze of PCB Common-Mode Radiation Based on Current-Driven Mode, *Work. Power Electron. Intell. Transp. Syst. IEEE.* 320 (2008).
24. M. Modarres, M.P. Kaminskiy, and V. Krivtsov, *Reliability Engineering and Risk Analysis* (CRC Press, 2009).
25. T. Sreenuch, A. Alghassi, S. Perinpanayagam, and Y. Xie, Probabilistic Monte-Carlo Method for Modelling and Prediction of Electronics Component Life, *Int. J. Adv. Comput. Sci. Appl.* 5 (2014).
26. K. Poorghasemi, R.K. Saray, E. Ansari, S.M. Mousavi, and A. Zehni, Statistical Analysis on the Effect of Premixed Ratio, EGR, and Diesel Fuel Injection Parameters on the Performance and Emissions of a NG/ Diesel RCCI Engine Using a DOE Method. *J. Automob. Eng.* 236, 460 (2022).
27. D. El Sherbiny and M.E.K. Wahba, OFAT versus DOE as Two Optimization Protocols for the Chromatographic Analysis of some OTC Pharmaceuticals Carrying Negative Cardiovascular Effects and Administered by Pregnant and Breast-Feeding Females: Application to dose Dependent Effect. *Acta Chromatogr.* 33, 11 (2020).
28. ŽR. Lazić *Design of Experiments in Chemical Engineering* (Wiley, 2004).
29. S. Bahrebar, and R. Ambat, Investigation of Critical Factors Effect to Predict Leakage Current and Time to Failure Due to ECM on PCB under Humidity. *Microelectron. Reliab.* 127, 114418 (2021).
30. S. Zhan, Surface Insulation Resistance of Conformally Coated Printed Circuit Boards Processed with No-Clean Flux. *Ieee Trans. Electron. Packag. Manuf.* 29, 217 (2006).
31. G. Grossmann and C. Zardini, *The ELFNET Book on Failure Mechanisms, Testing Methods, and Quality Issues of Lead-Free Solder Interconnects* (Springer, 2011).
32. M. Modarres, M. Amiri, and C. Jackson, *Probabilistic Physics of Failure Approach to Reliability* (Wiley, 2017).
33. S. Rastayesh, S. Bahrebar, A. S. Bahman, J. D. Sørensen, and F. Blaabjerg, Lifetime Estimation and Failure risk Analysis in a Power Stage Used in Wind-Fuel Cell Hybrid Energy Systems, *Electron.* 8 (2019).
34. O. El Aissaoui, Y. El Alami El, L. Madani, A.D. Oughdir, and Y. El Allioui, A Multiple Linear Regression-Based Approach to Predict Student Performance. *Adv. Intell. Syst. Comput.* 1102, 9 (2020).
35. M. Iwasaki, Multiple Regression Analysis from Data Science Perspective, *Adv. Stud. Behav. Data Sci*. 131 (2020).
36. P.V. Varde, and M.G. Pecht, *Probabilistic Approach to Reliability Engineering* (Springer, 2018).
37. M. E. N. H. and B. Peacock, Statistical Distributions, Third Edition, *Meas. Sci. Technol.* 12 (2001).
38. H. Rinne, *The Weibull Distribution : A Handbook* (Chapman & Hall/CRC, 2009).
39. S. Bahrebar, D. Zhou, S. Rastayesh, H. Wang, and F. Blaabjerg, Reliability Assessment of Power Conditioner Considering Maintenance in a PEM Fuel Cell System. *Microelectron. Reliab.* 88–90, 1177 (2018).
40. P.V. Varde and M.G. Pecht, *Risk-Based Engineering* (Springer, 2018).
41. N.T. Thomopoulos, *Statistical Distributions* (Springer, 2017).
42. K.C. Kapur and M. Pecht, *Reliability Engineering* (Wiley, 2014).
43. N. Matloff, *Statistical Regression and Classification* (Chapman and Hall CRC, 2017).
44. G. Giordano and M. Aria, *Regression Trees with Moderating Effects, New Perspectives in Statistical Modeling and Data Analysis* (Springer, 2011).
45. R.A. Berk, *Classification and Regression Trees (CART), Statistical Learning From a Regression Perspective* (Springer, 2016).
46. H. Huang, X. Guo, G. Zhang, and Z. Dong, The Effects of Temperature and Electric Field on Atmospheric Corrosion Behaviour of PCB-Cu under Absorbed Thin Electrolyte Layer. *Corros. Sci.* 53, 1700 (2011).
47. D. Berrar, Cross-Validation. *Encycl. Bioinforma. Comput. Biol. ABC Bioinforma.* 1–3, 542 (2019).
48. G. Jiang and W. Wang, Error Estimation Based on Variance Analysis of K-Fold Cross-Validation. *Pattern Recognit.* 69, 94 (2017).
49. E. K. Ampomah, Z. Qin, and G. Nyame, Evaluation of Tree-based Ensemble Machine Learning Models in Predicting Stock Price Direction of Movement, *Inf.* 11 (2020).
50. A. Debón, A. Carrión, E. Cabrera, and H. Solano, Comparing Risk of Failure Models in Water Supply Networks Using ROC Curves. *Reliab. Eng. Syst. Saf.* 95, 43 (2010).
51. Y. Jung, Multiple Predicting K-Fold Cross-Validation for Model Selection. *J. Nonparametr. Stat.* 30, 197 (2018).

52. S. Dahbi, H. El Moussami, and L. Ezzine, Multiple Regression Model for Surface Roughness Using Full Factorial Design, *Int. Conf. Ind. Eng. Syst. Manag. IEEE.* 439 (2016).
53. F.E. Harrell, *Regression Modeling Strategies* (Springer, 2015).
54. W.D. Dupont, *Statistical Modeling for Biomedical Researchers: A Simple Introduction to the Analysis of Complex Data*, 2nd ed., (Cambridge University Press, 2009).
55. B. Song, M.H. Azarian, and M.G. Pecht, Effect of Temperature and Relative Humidity on the Impedance Degradation of Dust-Contaminated Electronics. *J. Electrochem. Soc.* 160, C97 (2013).
56. A. Khangholi, F. Li, K. Piotrowska, S. Loulidi, R. Ambat, G. Van Assche, A. Hubin, and I. De Graeve, Humidity Robustness of Plasma-Coated PCBs. *J. Electron. Mater.* 49, 848 (2020).
57. W.S. Hong and C. Oh, Lifetime Prediction of Electrochemical Ion Migration with Various Surface Finishes of Printed Circuit Boards. *J. Electron. Mater.* 49, 48 (2020).
58. S. Joshy, V. Verdingovas, M.S. Jellesen, and R. Ambat, Circuit Analysis to Predict Humidity Related Failures in Electronics: Methodology and Recommendations. *Microelectron. Reliab.* 93, 81 (2019).
59. K. Lepenioti, A. Bousdekis, D. Apostolou, and G. Mentzas, Prescriptive analytics: literature Review and Research Challenges. *Int. J. Inf. Manage.* 50, 57 (2020).
60. M. Sun, H.G. Liao, K. Niu, and H. Zheng, Structural and Morphological Evolution of Lead Dendrites during Electrochemical Migration. *Sci. Rep.* 3, 3227 (2013).
61. D. Minzari, F.B. Grumsen, M.S. Jellesen, P. Møller, and R. Ambat, Electrochemical Migration of Tin in Electronics and Microstructure of the Dendrites. *Corros. Sci.* 53, 1659 (2011).
62. R. Ambat, H. Conseil-Gudla, and V. Verdingovas, *Corrosion in Electronics, Encyclopedia of Interfacial Chemistry* (Elsevier, 2018), p. 134.
63. H.W. Zhang, Y. Liu, J. Wang, and F.L. Sun, Effect of Elevated Temperature on PCB Responses and Solder Interconnect Reliability under Vibration Loading. *Microelectron. Reliab.* 55, 2391 (2015).
64. K. Piotrowska, R. Ud Din, F.B. Grumsen, M.S. Jellesen, and R. Ambat, Parametric Study of Solder Flux Hygroscopicity: Impact of Weak Organic Acids on Water Layer Formation and Corrosion of Electronics. *J. Electron. Mater.* 47, 4190 (2018).
65. K. Piotrowska, V. Verdingovas, and R. Ambat, Humidity-Related Failures in Electronics: Effect of Binary Mixtures of Weak Organic Acid Activators. *J. Mater. Sci. Mater. Electron.* 29, 17834 (2018).
66. K. Piotrowska and R. Ambat, Residue-Assisted Water Layer Build-Up Under Transient Climatic Conditions and Failure Occurrences in Electronics. *IEEE Trans. Compon. Packag. Manuf. Technol.* 10, 1617 (2020).